

# Melt Crystallization of Constrained Polyethylene Chains in Uniaxially Drawn Film and Solution-Grown Lamellae

Naoya Taniguchi and Akiyoshi Kawaguchi\*

Faculty of Science and Engineering, Ritsumeikan University, 1-1-1, Nojihigashi, Kusatsu, 525-8577 Shiga, Japan

Received October 14, 2004; Revised Manuscript Received February 14, 2005

**ABSTRACT:** When a uniaxially drawn polyethylene film was coated by evaporation of carbon in a vacuum, the deposited carbon layer fixed the texture and molecular orientation. Polyethylene single crystals were fixed at the fold surface on a carbon pedestal by carbon deposition. Since molecular chains of these samples were anchored on the carbon pedestal, their translational displacement on the pedestal, and longitudinal sliding along their axis, were largely restricted even when their thermal motions were activated at high temperatures. Consequently, the original molecular direction and the stacked lamellar morphology in drawn film, and the lozenge shape of polyethylene single crystals, were retained in the molten state. On crystallizing from melt, the stacked lamellar structure was reconstructed in the drawn film as double orientation was performed, and the *c* axis was parallel to the drawing direction, as the *b* axis was aligned preferentially parallel to the film surface. In single crystals, constrained chains crystallized in such a way that the *b* axis was kept in the lamellar plane, and their chain axis was tilted toward the long axis of the lozenge (the *a* axis) from the lamellar normal with an angle of 30°–54°.

## Introduction

Carbon evaporation in a vacuum has been widely used to make a thin supporting film of specimens for electron microscopy. Traditionally, the carbon-evaporation method has also been applied to replicate the surface of materials in one- or two-step process, to observe their fine surface topography in electron microscopy, until scanning electron microscopy, and later scanning probe microscopy, became popular for the purpose. In the one-step process of replication, a carbon thin layer was directly deposited onto materials by evaporation, and subsequently they were removed by dissolving in a solvent. In some cases, materials remained partly unresolved and transferred to the side of deposited carbon film. The carbon replica thus contaminated frustrated electron microscopists or polymer morphologists. Bassett has positively utilized the transfer of materials to carbon film and developed “detachment replication” to study the morphology of polyethylene (PE) single crystals.<sup>1</sup> It was found that polyethylene single crystals were transferred on the carbon film side when they were coated by carbon evaporation and that their morphology remained unchanged even after they were treated in a good solvent to remove uncoated crystals. Since then, detachment replication has been modified and utilized to observe the molecular orientation, as well as the topography of the surface, of thick specimens.<sup>2,3</sup> Recently, Yan et al. have utilized the ability of carbon coating and applied the method to fix the morphology and molecular orientation of drawn films of polymers.<sup>4–6</sup> The stacked lamellar morphology and molecular orientation in carbon-coated drawn film were kept after recrystallization from melt. It was found thus that carbon evaporation is of versatile use to fix the morphology and molecular orientation on material surface as well as to make a thin supporting film for electron microscopy. Here, we followed, in situ, the

morphological changes of thus carbon-coated PE specimens, i.e., drawn PE film and solution-grown single crystals, during heating, by using atomic force microscopy (AFM) with a polymer heating module. Supplementally, study on heat-treated samples by transmission electron microscopy (TEM) was carried out.

## Experiments

Specimens of uniaxially drawn, thin PE films and single crystals for AFM studies were deliberately prepared as follows.

A uniaxially drawn PE film for AFM observations was prepared by the method developed by Petermann and Gohil.<sup>7</sup> The thin PE film was put on a glass plate, and carbon was evaporated on it in a vacuum. Subsequently, the carbon-coated side of the PE film was fixed with an adhesive, Araldite, to protect against breaking down of the film by shrinkage with heating to a high temperature. The uncoated, opposite side of the film was examined by AFM (Nanoscope IIIa with a polymer heating module (Digital Instruments)). For TEM study, a drawn, thin PE film was picked up on a copper grid, and carbon was deposited on it by evaporation, as usual. The thin film thus prepared was annealed at various temperatures.

Figure 1 shows the procedure to prepare a PE single-crystal sample for AFM study. Polyethylene single crystals were grown by the self-seeding method.<sup>8</sup> A fractionated polyethylene with  $M_n = 32\,000$  ( $M_n/M_w = 1.1$ ) (No. 1483 product by NIST) was used. Polyethylene single crystals were put on a smooth surface, for example, on a glass plate for optical microscopy, and subsequently the glass surface was covered by a thin layer of 10% collodion solution in isoamyl acetate. After drying up the collodion solution, a collodion thin film was peeled off. Polyethylene single crystals were transferred to the collodion film. Carbon was deposited by evaporation onto the smooth surface of the collodion film in contact with the glass plate. In the next step, a piece of the thus prepared collodion film was put on a metal plate for AFM observation, and dipped in isoamyl acetate, to dissolve out the collodion.

In the above experiments, the thickness of the carbon layer was comparable to that of the supporting film for conventional electron microscopy, i.e., 20–30 nm.

\*To whom correspondence should be addressed: e-mail akiyoshi@se.ritsumei.ac.jp.

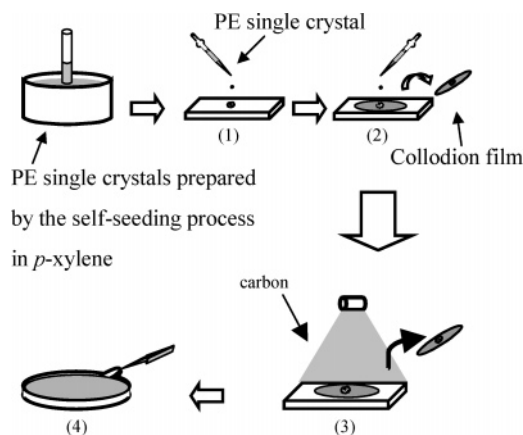


**Figure 1.** Scheme of the preparation process of a carbon-coated polyethylene single-crystal sample for AFM. (1) A drop of a suspension of polyethylene single crystals in xylene was put on a glass plate and dried up. (2) The glass plate was covered with a thin layer of 10% collodion solution in isoamyl acetate. (3) After drying up, the collodion film was peeled off, turned over, and fixed on a glass plate. Thereafter, the collodion film surface in contact with the glass plate was coated with carbon. (4) A piece of carbon-coated film was put on a copper grid for transmission electron microscopy, and on a metal plate for AFM, with the carbon-coated side in contact with them. Subsequently, collodion was dissolved away in isoamyl acetate.

## Results

**A. Carbon-Supported, Uniaxially Drawn Polyethylene Film.** Figure 2 shows AFM height images of a carbon-coated drawn film, which were recorded in situ at the indicated temperatures. An as-prepared, unannealed sample is composed of edge-on lamellae, which are stacked with their long axis perpendicular to the drawing direction (see Figure 2a). Figure 2b was taken in situ at 140 °C. The textural features as observed at room temperature in Figure 2a are still recognized in Figure 2b: The edge-on “lamellae” are stacked, and striations run vertically. As the present observation temperature was “apparently” above the melting point, polyethylene should be molten. However, the followings should be inquired in interpreting the morphology of Figure 2: (1) did superheating not occur, and (2) was it experimentally assured that the “surface temperature” was as high as indicated here? As we see from monograph by Wunderlich,<sup>9</sup> superheating is serious in interpreting the melting point of polymer crystals, especially from the dynamical measurement such as DSC. When the drawn PE constrained by fixing the length was heated, it showed superheating.<sup>10</sup> In the present experiments, however, there is no problem on superheating in terms of dynamical process because it took more than 5 min to take an image, during which polymer chains could be relaxed. When constrained chains such as tie molecules in the amorphous domain of drawn PE were carbon-coated, chains could be constrained more, and hence the melting point might increased because the entropy change of fusion of constrained chains could be smaller than that of unconstrained chains.<sup>11</sup> However, this is not discussed further here in lack of concerning data. The second inquiry is serious: Schönherr et al.<sup>12</sup> have observed that there was considerable temperature difference between the calibrated temperature of instrument and true surface temperature, which reached several degrees depending on the atmospheric gas. We have no data of surface temperature measured directly by other methods. Actually, height AFM images was not

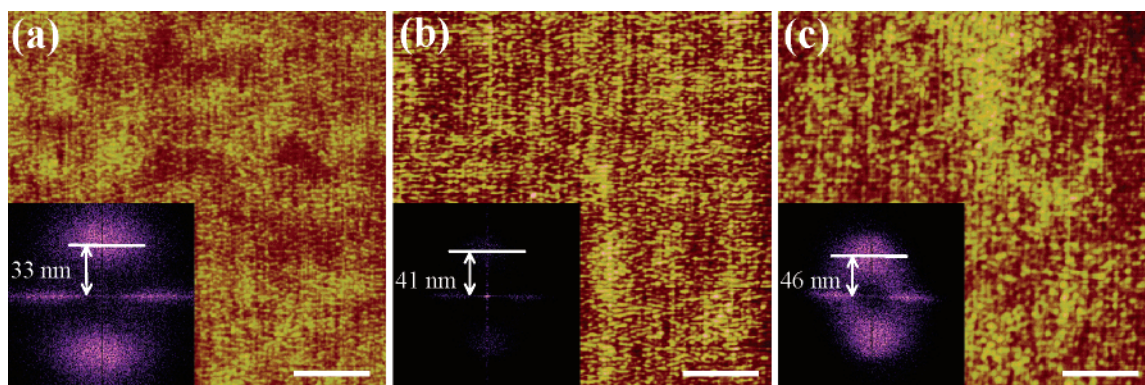
able to be obtained at a temperature as high as 150 °C because the sticky force of Si probe to molten PE became so much strong. However, the height image, exhibiting the same morphological characteristics as in Figure 2b, was still recorded at a temperature of 145 °C, though image quality was reduced. Empirically, we considered the surface temperature is not so lower than the temperature indicated on the AFM heating module, judging from the following observations: In the present work and the work by Nakamura and Kawaguchi<sup>13</sup> on annealing PE single crystals, the morphology of PE single crystals largely changed at a temperature comparable to that as reported so far and that *n*-alkane C<sub>36</sub>H<sub>72</sub> (mp 73–75 °C) melted down at about 75 °C. It is concluded, thus, that polyethylene was molten or just below the melting points in Figure 2b, still preserving a stacked texture of “noncrystalline” lamellae.

When a drawn PE film fixed simply by Araldite substrate, without carbon coating, was melted, the resultant melt condensed into droplets. The morphology of molten polyethylene was quite different between with and without a carbon coating. It is to be stressed that a carbon coating effectively functioned to retain the stacked lamellar texture, which was originally formed in drawn PE, even after polyethylene was melted. Figure 2c shows the AFM height image, which was taken after cooling to room temperature from 150 °C. After recrystallization, a surface topography quite similar to that before annealing is reproduced (cf. Figure 2a).

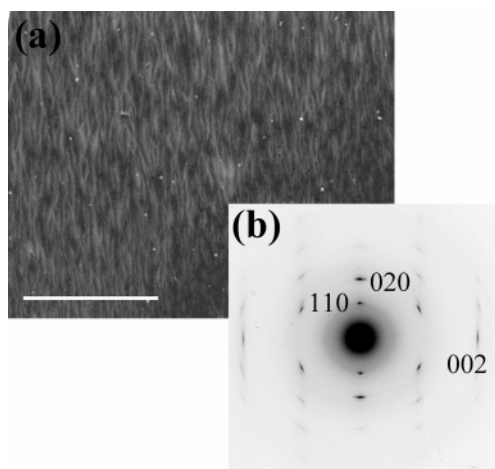
The insets in Figure 2 show digital Fourier transforms, each of which was obtained from the corresponding phase images to the respective height images. Of course, the Fourier transforms can be obtained from the height images in Figure 2. However, the discrete “scatterings” are not as intense as in the insets, although features similar to those of transforms are recognized. To emphasize the scattering features, the transforms corresponding to the phase images are adopted here. The scattering features are as follows: (1) Discrete scattering is observed. (2) The long periods, which are evaluated from the peak position of discrete scattering of Figure 2b,c, are larger than that of Figure 2a; the long period of Figure 2a is 33 nm, and those of parts b and c of Figure 2 are 41 and 44 nm, respectively. (3) The intensity of discrete scattering of Figure 2b is weaker than those of Figure 2b,c. Comparing the height image of Figure 2b with that of Figure 2a, we perceive that the stacked lamellae thicken in the molten phase. The discrete scattering confirms this. It is common that, when polyethylene is drawn at a rather high temperature, a long period is caused in the drawn polymer, depending on the drawing temperature.<sup>14</sup> The long period seen in Figure 2a is usual. However, the long period value of as-drawn film is not assessed appropriately because the drawing temperature is unknown. The increased long period was preserved after recrystallization; roughly identical long periods are observed in Figure 2b,c. Feature 3 indicates that the stacking order of molten lamellae should become poorer. In addition, it implies that the surface could be more even in the molten phase: we explain that in X-ray or electron diffraction by real materials, the decreased intensity may be due to less fluctuation of electron density, which may correspond to the surface evenness.

Figure 3 shows an electron micrograph and the corresponding electron diffraction pattern of a carbon-





**Figure 2.** Height images of a carbon-coated drawn film, taken at (a) room temperature, (b) 140 °C, and (c) room temperature after recrystallization from melt after being heated at 150 °C. The scale bar denotes 0.5  $\mu\text{m}$ . The drawing direction is vertical. The insets are the digital Fourier transforms obtained from the phase images corresponding to the respective height images (see text). All images are 256  $\times$  256 pixels wide.



**Figure 3.** (a) Electron micrograph and (b) the corresponding electron diffraction pattern. These were taken at room temperature after cooling. The drawing direction is horizontal. The scale bar corresponds to 5  $\mu\text{m}$ .

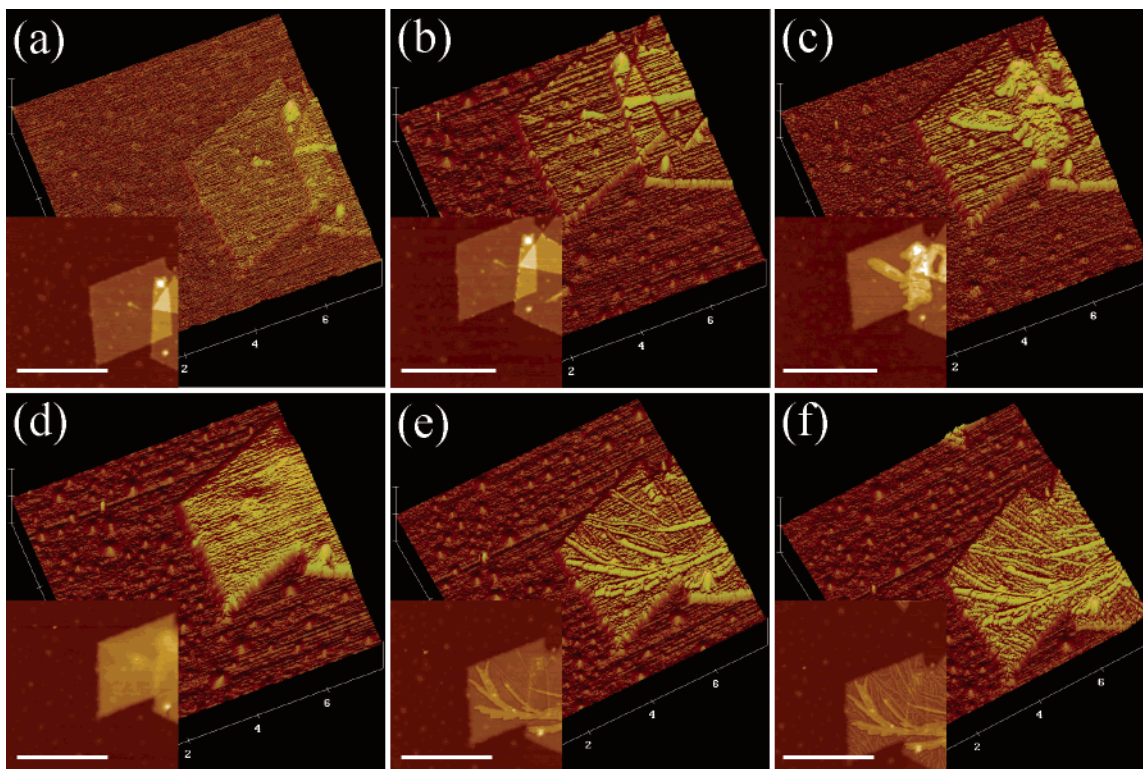
coated, drawn, thin PE film, which was heat-treated at a temperature above the melting point, e.g., 140 °C. Morphological and diffraction features described in reports by Shouke et al. are recognized: (1) Lamellae are stacked with their long axis perpendicular to the drawn axis. (2) The 020 reflection is strong, and the 200 reflection disappears, with the *c* axis orientation being kept. In some cases, the 110 reflection disappears (cf. Figure 3b).<sup>4,5</sup> The morphological feature manifests itself more clearly in the above AFM images. However, it must be taken into account that the AFM image shows the surface topography, and the electron micrograph corresponds to the projected electron density fluctuation. The diffraction feature 2 shows that PE crystallites are doubly oriented with the preferred orientation of the *b* axis parallel to the film surface. When a carbon-coated PE drawn film was annealed below the melting point, it did not exhibit the *b* axis orientation, although the degree of double orientation increased.<sup>15</sup> The preferred *b* axis orientation results from and is characteristic of melt crystallization.

**B. Annealing of Carbon-Pedestaled Single Crystals.** Usually, when polymer single crystals are put on a thin carbon-supporting film for electron microscopy, they are deposited in a convex form on it. To keep the convex deposition and fix the bottom fold surface of PE single crystals on a carbon pedestal, the present elaborated procedure was adopted as detailed in the experi-

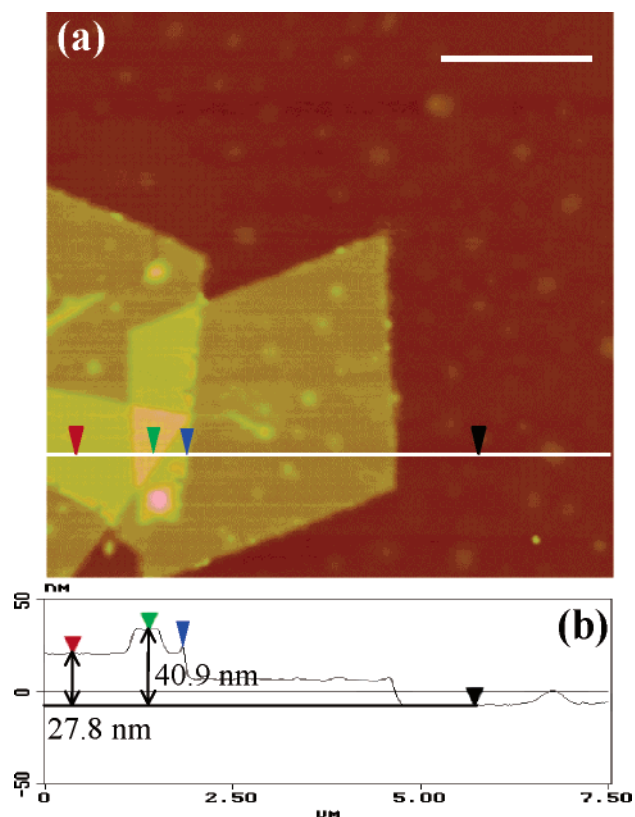
mental section. The convex deposition is an advantage experimentally, in that lamellar thickness can be followed on heating by AFM.

Figure 4 shows a series of AFM height images of polyethylene single crystals settled on a carbon pedestal, which were taken in situ at the indicated temperatures in a heating and cooling cycle. Figure 4a shows clearly that PE single crystals were pedestaled on in a convex form. The lozenge shape of PE single crystal was deformed into an indefinite form when it was simply put and melted on carbon substrate. It was examined in detail by AFM as to how PE single crystals change their morphology in the process of heating on carbon substrate, when they are put simply on carbon substrate.<sup>13</sup> Figure 4d was taken in situ at 140 °C. The image demonstrates plainly that the lozenge form of PE single crystals was still maintained even after they were heated to a temperature above the melting point. It is also distinctive that no holes were produced in lamellae. It is affirmed that the bottom fold surface of single crystals was firmly fixed on a carbon pedestal, which was deposited by evaporation in a vacuum, and correspondingly, the original shape in the crystalline state could remain undeformed.

When PE single crystals were only deposited on carbon substrate and heated to higher temperatures, various morphologies were exhibited in the process of heating.<sup>13</sup> Here, we shall focus on two interesting morphological behaviors that carbon-coated lamellae exhibited during heating. The first is seen in Figure 5, which shows a magnified AFM height image corresponding to Figure 4b, and the line profile scanned along the line in the image. Here, three lamellae are stacked in the form of a staircase. The staircase height profile traces two jumps in height, each of which corresponds to the step height of a lamella. The changes in height of respective terraces from the pedestal surface are plotted in Figure 6. The top terrace bulges at both edges. The increment from the plateau is appreciably smaller than that at the edge indicated by the blue mark. From this, we see the stacking order of three stacked lamellae: The triangle region of three overlapping lamellae is in the middle; that is, the lozenge protruding from the lower left is sandwiched by other lamellae. This is because when lamellae are free in space, they thicken first and easily at the periphery. It is considered, further, that when lamellae are confined between two lamellae, thickening could be restrained and retarded even at their edge compared with in a spatially free



**Figure 4.** Landscape AFM height images, with the corresponding projected images, taken in situ at (a) room temperature before heating, (b) 120 °C, (c) 125 °C, and (d) 140 °C in the heating process and at (e) 110 °C and (f) 80 °C during cooling. The insets are the projected AFM images. The scale bars denote 4  $\mu\text{m}$ . All image are 256  $\times$  256 pixels wide.



**Figure 5.** (a) Enlarged AFM height image of Figure 4b and (b) the height profile obtained by scanning along the line in the image. The positions marked with left and right triangles in (a) correspond to those in (b). Scale bar denotes 5  $\mu\text{m}$ . All images are 256  $\times$  256 pixels wide.

lamella. Thus, it is understood that thickening is not so large at both edges at the top terrace, as follows: The

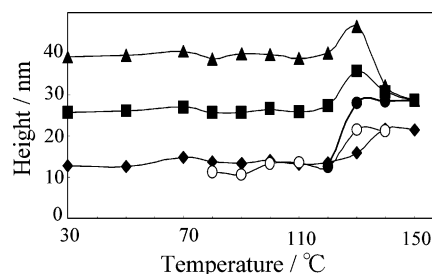


**Figure 6.** Heights of the staircase terraces, scanned along the line in Figure 5, as a function of observation temperature. Symbols  $\blacktriangle$ ,  $\blacksquare$ , and  $\blacklozenge$  denote the heights at the top, middle, and bottom terraces from the base, respectively. Symbols  $\bullet$  and  $\circ$  denote the heights of two regions in the cooling process: one region, in which multilamellae were stacked before melting, and the other, originally consisting of a single lamella. Because the height is fluctuated, all the values below 125 °C are heights for the highest population of height histogram. See the height histogram in Figure 8. However, heights of top and middle lamellae at temperature above 125 °C in the heating process were measured by local average.

left edge belongs to the bottom lamella and the right one to the middle triangular lamella.

Figure 6 shows the heights of top, middle, and bottom lamellar terraces of the staircase from the carbon pedestal as a function of observation temperature. Jumps of terrace height correspond to the thickness of a lamella. The thicknesses of these lamellae are identical. As seen in Figure 4c, the top and middle lamellae were melted down and fused at ca. 125 °C. Correspondingly, the thickness of the fused lamella decreased, and the thicknesses of the two lamellae are indistinguishable. As judged from the individual terrace heights, the lamellar thickness increased slightly up to ca. 125 °C, at which free lamellae were partially melted down. However, the bottom lamellae has a definite thickness



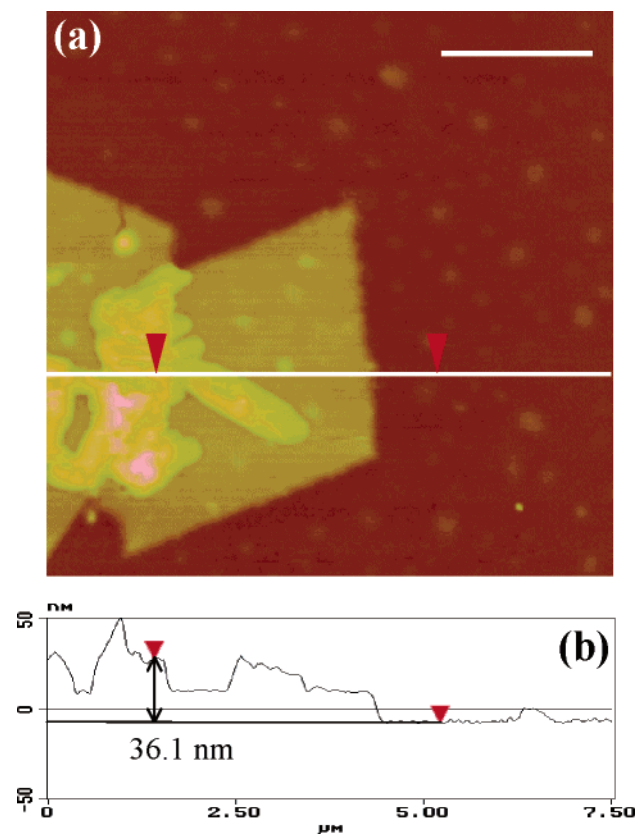


**Figure 7.** (a) Enlarged AFM height image of Figure 4c and (b) the height profile scanned along the line in the image. Scale bar denotes 5  $\mu\text{m}$ . Image is 256  $\times$  256 pixels wide.

above 125  $^{\circ}\text{C}$ , which increases with increasing temperature and becomes larger by about 8 nm than the thickness below the temperature. When PE single crystals were annealed on carbon substrate, the lamellar thickness increased with increasing temperature, as they thickened in advance at their periphery.<sup>13</sup> It is to be noted here that, even when a crystalline PE lamella was transformed into a “molten lamella”, it had a definite thickness that increased a little compared with the crystalline lamellar thickness at room temperature. It is considered that the molten lamellae were composed of normally standing chain stems, the length of which was roughly identical to that in the crystalline phase, and consequently, their surface remained smooth. We confirm again that polyethylene chains should be anchored at their folds on the carbon pedestal by carbon coating, so that chains cannot displace or slide to form thicker lamellae. Further, we notice an interesting phenomenon of a decrease in lamellar thickness in the cooling process: The heights (corresponding to the lamellar thickness) of two regions, which were formed of multilayered and single lamella(e) before melting, decreased drastically to an identical value, i.e., about 12 nm, around 125  $^{\circ}\text{C}$ , at which crystallization occurred. It is interesting that the averaged thickness of rough surface is almost the same as that of original crystalline lamellae.

Figure 7 shows an enlarged AFM image of Figure 4c. The bottom lamella, which is fixed to the carbon pedestal, did not deform but retained the original shape at 125  $^{\circ}\text{C}$ . However, both middle lamellae, sitting on the carbon-pedestaled lamella, and the top lamella on it, were deformed and lost their original appearance due to partial melting above the temperature. They were

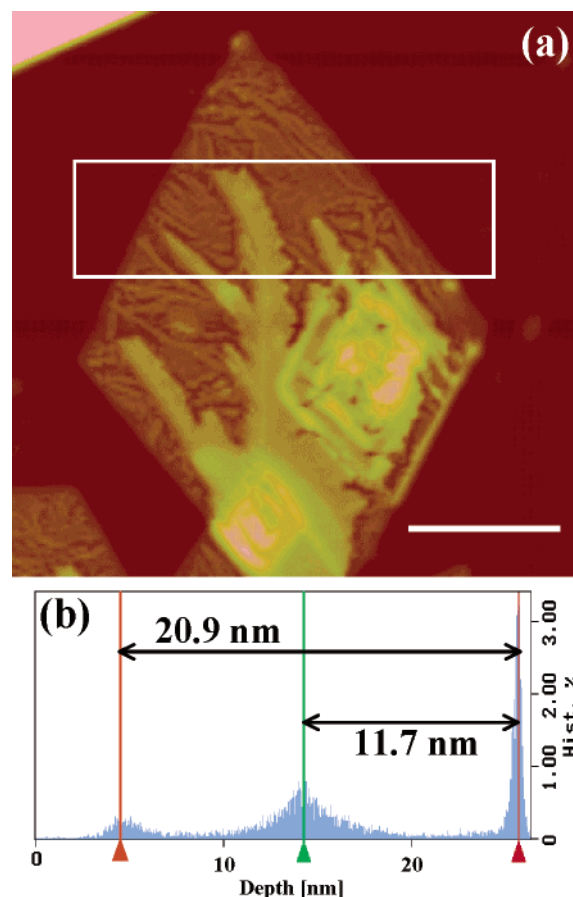


**Figure 8.** (a) AFM height image of carbon-coated, annealed PE single crystals, which had originally a spiral terrace. Scale bar denotes 5  $\mu\text{m}$ , and image is 256  $\times$  256 pixels wide. (b) Height histogram of the rectangularly enclosed area in (a).

fused and spread over the surface of the bottom lamellae, forming a layer. It is noteworthy here that the transiently produced polyethylene melt could spread readily over on the smooth surface of polyethylene substrate.

Figure 8 shows another AFM image featuring annealed, carbon-coated PE single crystal, taken at room temperature. As seen in Figure 4f, the lozenge was kept as well, and fine fibrils and blobs were formed in an irregular fashion. They are crystalline, as shown below by electron diffraction. However, the molecular orientation in respective fibrils and blobs is undefined. As seen in the histogram, we see again that the bottom lamella has a height as large as 11.7 nm, which is slightly smaller than that of an original lamella (12.5 nm) and is rather smooth with a fluctuation within a few nanometers. In Figures 4 and 7, lamellae sitting on the pedestaled lamella spread over it and deformed in indefinite shape. In comparison with it, it is to be noted that the edge of spiral terrace can be traced, although the entire spiral terrace morphology was destroyed due to flowing out of uncoated lamellae. The spiral terrace of PE lamellae, which was fixed by carbon coating, was retained when treated in hot xylene.<sup>1</sup> In the same way, the carbon-coated terraces remain in the molten state. Recrystallization could occur at the terrace to restore the original terrace structure.

Figure 9 shows an electron micrograph and the corresponding electron diffraction pattern of a PE single crystal, which was fixed on the carbon pedestal and annealed at 140  $^{\circ}\text{C}$ . The electron diffraction pattern is

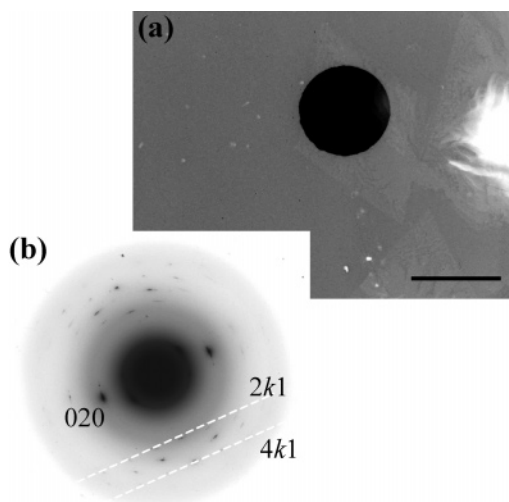


**Figure 9.** (a) Electron micrograph of a carbon-pedestaled polyethylene single crystal, which was annealed at 140 °C, and (b) the corresponding electron diffraction pattern. The scale bar corresponds to 3  $\mu\text{m}$ . Notations  $2k1$  and  $4k1$  show the reflection sets along the white dotted lines.

indexed suitably as shown in Figure 10a. Of  $hk0$  reflections, the strong 020, and its higher order reflection 040, were observed in the direction parallel to the short diagonal (the  $b$  axis) of the lozenge. In addition, sets of  $2k1$ ,  $3k1$ ,  $4k1$ , and  $5k1$  reflections were observed in a layer line. In some case, however, only the  $2k1$  set of reflections was strongly observed, and in other cases, only the  $4k1$  set of reflections, intensively, while the 020 reflection was always retained in the same way as above. However, there was no observation, solely, of any of  $3k1$  and  $5k1$  sets of reflections. The electron diffraction patterns explain that the chain axis was tilted from the normal to the lamellar surface toward the long diagonal (the  $a$  axis) of the lozenge, keeping the  $b$  axis parallel to the pedestal surface. Since all the sets of reflections never fulfill the reflection condition simultaneously, it is clear that many crystallites, e.g., blobs and fibrils, in which PE chains were tilted with a different inclination angle were produced. However, the molecular inclination in individual blobs and fibrils is unknown.

## Discussion

It was found that the carbon coating fixed the PE morphology, retaining the original molecular orientation, even when PE was melted at a temperature above the melting point. It is considered to be fixed in the following way: Evaporated carbon, which may be atomic or nanosize particles, may be so reactive that it can chemically bond with polymer chains, and otherwise, polymer chains could be embedded in the deposited carbon layer; that is, evaporated carbon particles could diffuse into the polyethylene solid, especially into the amorphous region, to form a carbon matrix including polymer chain in it.<sup>1,6</sup> When the PE film was fixed with Araldite adhesive, polyethylene chains could also be embedded in the matrix. However, the chains were not fixed in the molten state because polyethylene melted into droplets and because spherulites were grown on it when the sample was recrystallized from melt. It seems less possible that polyethylene chains could be anchored by embedding in the substrate matrix, although the following must be taken into account in consideration: The individual adhesive macromolecules might not

penetrate deeply into polyethylene solid, and the interaction between polyethylene molecules and the adhesive molecules might not be so strong. At any rate, it was made clear, here, that carbon-coated PE samples exhibited the following characteristics by annealing: (1) The original morphology of polyethylene, i.e., the stacked lamellar structure of uniaxially drawn film and the lozenge shape of polyethylene single crystals, was preserved in the molten phase. (2) The  $c$  axis molecular orientation was fixed in the drawn film.<sup>4</sup> (3) Crystallization from melt caused the preferred orientation of the  $b$  axis (a) parallel to the film surface of drawn film and (b) parallel to the short diagonal (the  $b$  axis direction) of the original lozenge of single crystals. Polyethylene chains were anchored at the fold parts on carbon pedestal in single crystals. The anchored molecular chains could not displace on the pedestal and slide along their axis, although their molecular motions are activated thermally at higher temperatures. Thus, it is easily understood that the lozenge shape of single crystals can be retained in the molten state. As seen in Figure 4c, however, molecular chains less entangled in solution-grown, unfixed lamellae were able to move rather freely on the surface of the underlying, fixed lamella. In contrast, the structure of the drawn film is so complicated, as modeled in ref 16: The stacked lamellae might be interlinked by tie chains; molecular chains might fold with long loose loops, and so on. Thus, it is conceived that the complication could result in largely entangled chains in the molten state, and hence they could not move around so easily as in single crystals that the stacked lamellar structure would be remain in the molten state.

Molten chains tend to take a randomly coiled conformation. When a crystalline lamella is melted, its shape could be shrunk in the length direction, and expanded in the thickness direction, so that the lamellar form could be changed to an oval one due to melting. Such a change in lamellar form is observed in comparing Figure 2b with Figure 2a. Thus, the larger long period in Figure 2b is understood in terms of the expansion of molten lamellae in the drawing direction. The larger long period was retained after recrystallization. It is usual for the long period of melt-crystallized sample to be larger, depending on the crystallization temperature.

The electron diffraction pattern in Figure 9a is explained on the basis of the Ewald construction of reflection, as shown in Figure 10b. For the  $4k1$  set of reciprocal lattice points to be put on the Ewald sphere of reflection (nearly flat plane for electron diffraction), the  $c^*$  axis must be tilted by 36° from the incidence of electron beams, while the  $b^*$  axis is kept in the sphere. In real space, the  $c$  axis—the chain axis—is tilted by 36° from the normal to the lamellar surface, while the  $b$  axis lies in the lamellar plane. For the  $5k1$ ,  $3k1$ , and  $2k1$  sets of reflections to be observable, the chain axis must be tilted by 30°, 46°, and 54°, respectively. As seen in Figure 4f, carbon-pedestaled crystalline PE lamellae consist of fibrils or small blobs. The molecular orientation or inclination angle in fibrils and blobs may be changed from fibril to fibril and from blob to blob.

Originally, polyethylene chains stand almost perpendicular to the lamellar surface of polyethylene single crystals, as deposited on substrate. As discussed above, carbon-pedestaled molten lamellae consist of normally standing chain stems. It is unknown whether the thickness of molten lamellae corresponds to the stem

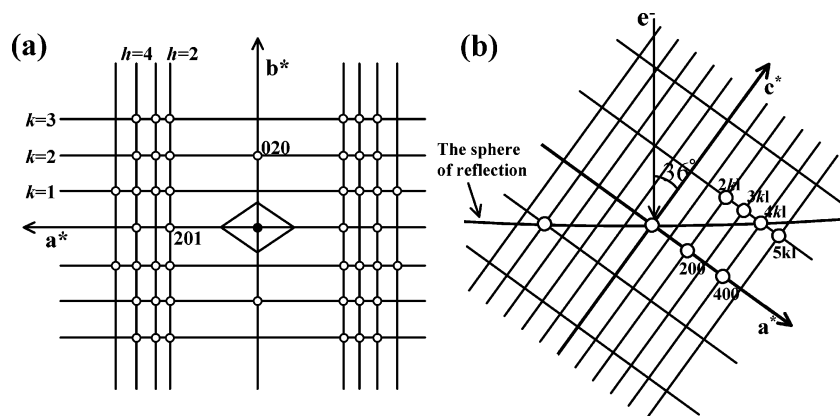


**Figure 10.** (a) Schematic drawing of the electron diffraction pattern of Figure 9b. A lozenge is drawn to show the orientational relationship between the electron diffraction pattern and a polyethylene single crystal. (b) Ewald construction for reflection for electron diffraction giving the  $4k1$  set of reflections, projected on the  $a^*-c^*$  plane.

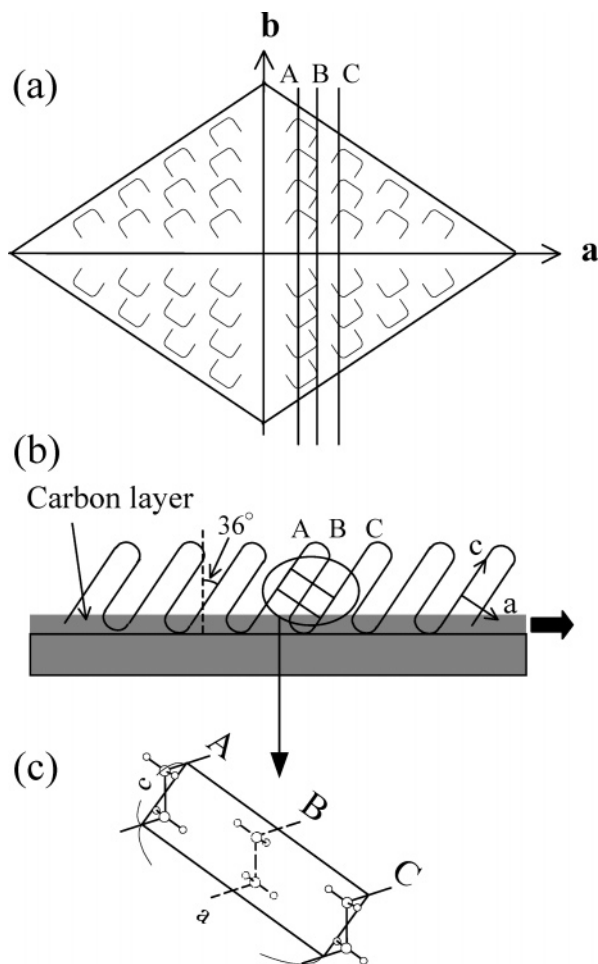


**Figure 11.** (a) Schematic top view of lamella. (b) Lamellar model of tilted chains with a tilting angle of  $36^\circ$ , viewed down the  $b$  axis; that is, the short diagonal of lamella. Thick arrow denotes the direction of long diagonal of lozenge (the  $a$  axis). (c) The detailed sketch of unit cell encircled in (b). A, B, and C in (b) and (c) denote the projected chain arrays, viewed down the  $b$  axis in (a).

length. The tilting of molecular chains in recrystallized lamella can be explained on the basis of the molecular arrangement, as depicted in Figure 11 with the tilting angle of chains of  $36^\circ$ , in which the  $4k1$  set of reflections is observable. Arrays of chain stems, which are aligned along the  $b$  axis (see Figure 11a), are shifted progressively in the direction parallel to the chain axis by the distance  $n \times (c/2)$ , where  $n$  is an integer and  $c$  is the  $c$

dimension of the unit cell, with respect to their neighboring array (see Figure 11b). For example, in the model with  $n = 2$ , the chain array of B is shifted by the  $c$  dimension distance with respect to the array of A, the array C with respect to the array B, and so on. The angles of  $30^\circ$ ,  $46^\circ$ , and  $54^\circ$  are performed by shifting for  $n = 1, 3$ , and  $4$ , respectively; the neighboring chain arrays, e.g., arrays A and B, are shifted progressively by the length of 1, 3, and 4 time(s) the  $c/2$ , respectively. The shifting for  $n = 2$  and  $4$  means that the neighboring arrays of chains are shifted progressively along their chain axis, one after another, by a length of once and twice the  $c$  dimension of the unit cell. In even number shifting mode, thus, the orthorhombic subcell packing of chain stems is always performed by simply shifting of the length. However, for odd number shifting, e.g.,  $n = 1$  and  $3$ , the orthorhombic unit cell packing could not be achieved only by progressive shifting. We see from Figure 11c that the orthorhombic subcell is not performed by shifting when the array B is shifted by half the unit cell length or by one and half with respect to the array A. In addition, the chains in the array B should be rotated by about  $90^\circ$  about their chain axis to maintain the orthorhombic unit cell. This shows only the crystallographic requirement to maintain the orthorhombic unit cell, but not the crystallization mechanism. On the basis of the chain tilting occurring in this way, the observed electron diffraction pattern can be explained. This proves, at least, that chain tilting should be given rise to as a crystallographic consequence on crystallization of constrained chains.

When solution-cast PE films, consisting of single crystals, were annealed, molecular chains in them were rotated about the  $b$  axis and tilted toward the  $a$  axis, by up to  $56^\circ$ , which is just comparable with the present value.<sup>17</sup> When polyethylene is crystallized from melt, it exhibits various types of lamellar morphology, viewed down the  $b$  axis: we list ridge, planar sheet, and S types.<sup>18,19</sup> In the various types of lamellae, molecular chains are tilted from the normal to the lamellar surface, to give  $\{201\}$  facets. The tilting angle of molecular chains from the surface normal is  $34^\circ$ , just corresponding to the present tilting with  $n = 2$ . It was also observed that polyethylene chains were tilted at the same angle in thin polyethylene lamellae, which were grown in solution at high temperature and largely extended in the  $b$  axis direction.<sup>20</sup> In molten, pedestaled PE lamellae, molecular chains should be fixed at the fold surface, i.e., at one end of molecular stems, but they



should be originally registered suitably for crystalline ordering. It is considered that, when constrained molecular chains are crystallized from melt, they are forced to form a crystalline plate, taking on the morphological feature with the above-mentioned relationship of chain orientation to the lamellar surface. Then, the pedestaled fold surface would have to become the {201} plane, and the molecular chains tilt toward the  $a$  axis because the  $b$  axis is registered to the short diagonal. It is made clear that, when PE lamellae grow through the multiple secondary nucleation process, their shape is elongated in the direction parallel to the  $b$  axis.<sup>21–23</sup> Future study will have to determine how the growth mechanism of elongated lamellae could be concerned with the crystallization of the constrained molecules, to achieve the present preferred  $b$  axis orientation.

The as-drawn film was basically polycrystalline, as the fiber electron diffraction shows. In the sample, some constituent crystallites were oriented, for example, with their  $b$  axis normal to the film surface and others with the  $a$  axis. When the sample was carbon-coated, polyethylene chains in the carbon-sample boundary could memorize their orientation and conformation in the original texture. When crystallization occurred in the boundary region, chains would reorganize the original structure, restoring their original arrangement. If so, crystallites with the  $a$  axis parallel to the substrate surface could be reproduced. In reality, only the  $b$  axis orientation to the film surface is realized preferentially. It is unknown how this molecular orientation is related to that in carbon-coated polyethylene single crystals.

### Concluding Remarks

The carbon pedestal, which was made by evaporation–deposition on drawn polyethylene film and polyethylene single crystals, anchored molecular chains on it. As a result, the original morphology was able to be maintained even when the constituent crystallites were melted. When the thus-constrained PE chains were recrystallized from melt, they restored the original molecular direction although the crystallographic  $a$  axis of chains were not restored. The characteristic, preferred  $b$  axis orientation was given rise to both in recrystallized drawn film and in melt-crystallized single crystals. However, it is unknown how the preferred  $b$  axis is related to the radially oriented  $b$  axis in melt-grown polyethylene spherulites and elongated lamellae grown from concentrated solution.

In the detachment replication by Bassett, carbon-coated polyethylene single crystals were treated in xylene at a temperature of as high as 95 °C, at which unfixed polyethylene single crystals were dissolved out.<sup>1</sup> The resultant carbon-coated polyethylene lamellae produced the  $hk0$  net electron diffraction pattern. When carbon-coated, drawn PE film was treated in hot xylene

as well, it gave a fiber pattern in electron diffraction, which was similar to that of an as-drawn sample.<sup>6</sup> It is certain that the solution-crystallization process of constrained chains was involved in both heat treatments in the solvent. We see that constrained molecular chains in carbon-coated polyethylene single crystals should take a different orientation when they crystallize from melt compared with from solution. This difference in molecular orientation implies that the crystallization mechanism differs between from melt and from solution. This question is open for future study. However, though there are some unknown phenomena of change in molecular orientation, this carbon coating would be valuable technically, in that the textural topography of polyethylene could be kept after being melted.

**Acknowledgment.** This study was partly supported by a Grant-in-Aid for Scientific Research on Priority Areas: “Mechanism of Polymer Crystallization” (No. 12127207) and partly by the High Technology Research Project 2001, from the Ministry of Education, Culture, Sports, Science, and Engineering.

### References and Notes

- (1) Bassett, D. C. *Philos. Mag.* **1961**, *6*, 1053–1056.
- (2) Pennings, A. J.; van der Mark, J. M. A. A.; Kiel, A. M. *Kolloid Z. Z. Polym.* **1970**, *237*, 336–368.
- (3) Monobe, K.; Fujiwara, Y.; Yamashita, Y. *Kogyo Kagaku Zasshi* (in Japanese) **1970**, *73*, 1420–1432.
- (4) Yan, S.; Katzenberg, F.; Petermann, J. *J. Polym. Sci., Part B* **1999**, *37*, 1893–1898.
- (5) Yan, S.; Lieberwirth, I.; Katzenberg, F.; Petermann, J. *J. Macromol. Sci., Part B* **2003**, *43*, 641–652.
- (6) Yan, S. *Macromolecules* **2003**, *36*, 339–345.
- (7) Petermann, J.; Gohil, R. M. *J. Mater. Sci.* **1979**, *14*, 2260–2263.
- (8) Blundell, D. J.; Keller, A.; Kovacs, A. I. *Polym. Lett.* **1966**, *4*, 481–486.
- (9) *Macromolecular Physics*; Wunderlich, B., Ed.; Academic Press: New York, 1980; Vol. 3.
- (10) Illers, K.-H. *Angew. Makromol. Chem.* **1970**, *12*, 89.
- (11) Zachmann, H. G. *Kolloid Z. Z. Polym.* **1965**, *206*, 25.
- (12) Schönherr, H.; Bailey, L. E.; Frank, C. W. *Langmuir* **2002**, *18*, 490–498.
- (13) Nakamura, J.; Kawaguchi, A. *Macromolecules*, in press.
- (14) Peterlin, A.; Corneliussen, R. *J. Polym. Sci., Part A-2* **1968**, *6*, 1273–1282.
- (15) Yang, D. C.; Thomas, E. L. *J. Mater. Sci.* **1984**, *19*, 2098–2110.
- (16) Hosemann, R. *J. Appl. Phys.* **1963**, *34*, 25–41.
- (17) Bassett, D. C.; Keller, A. *J. Polym. Sci.* **1959**, *40*, 565–568.
- (18) Bassett, D. C.; Hodge, A. M.; Olley, R. H. *Faraday Discuss. Chem. Soc.* **1979**, *68*, 217–224.
- (19) *Principles of Polymer Morphology*; Bassett, D. C., Ed.; Cambridge University Press: London, 1981.
- (20) Khoury, F. *Discuss. Faraday Chem. Soc.* **1979**, *68*, 404–405.
- (21) Toda, A. *Polymer* **1991**, *32*, 771–780.
- (22) Point, J. J.; Villers, D. *J. Cryst. Growth* **1991**, *114*, 228–238.
- (23) Toda, A. In *Crystallization of Polymers*; Dosièrè, M., Ed.; Kluwer Academic Press: Dordrecht, 1992; pp 141–152.

MA047869C